Chiroptical study of cryptophanes subjected to self-encapsulation

Orsola Baydoun, Thierry Buffeteau, Nicolas Daugey, Marion Jean, Nicolas Vanthuyne, Laure-lise Chapellet, Nicolas de Rycke, Thierry Brotin

Chiroptical Study of Cryptophanes Subjected to Self-Encapsulation

Orsola Baydoun,[†] *Thierry Buffeteau*[*,‡] *Nicolas Daugey,*[‡] *Marion Jean,*[§] *Nicolas Vanthuyne,*[§] *Laure-Lise Chapellet,*[†] *Nicolas De Rycke*[†] *and Thierry Brotin,*[*,†]

[†] Lyon 1 University, Ecole Normale Supérieure de Lyon, CNRS UMR 5182, Laboratoire de Chimie, 69364 Lyon, France

[‡] Bordeaux University, Institut des Sciences Moléculaires, CNRS UMR 5255, 33405 Talence, France

[§] Aix-Marseille University, CNRS, Centrale Marseille, iSm2, Marseille, France

e-mail: thierry.buffeteau@u-bordeaux.fr; thierry.brotin@ens-lyon.fr

Table of contents :

Figure S14: ^{1}H NMR spectrum (300 MHz) of (rac)-**2** recorded in $CDCl_3$ at 25 °C.

Figure S15: ^{1}H NMR spectrum (300 MHz) of (rac)-**2** recorded in 1,1,2,2-tetrachloroethane-d_2 at 25 °C.

Figure S16: ^{1}H NMR spectrum (300 MHz) of (rac)-**2** recorded in benzene-d_6 at 25 °C.

Figure S17: Specific Optical Rotation (SOR) values measured for [CD(+)$_{254}$]-**1** and [CD(−)$_{254}$]-**1** in CH_2Cl_2 (black), $CHCl_3$ (orange), DMSO (blue) and $C_2H_2Cl_4$ (red) at 25 °C. Plot of the SOR (10^{-1} deg cm^2 g^{-1}) values versus λ (nm) for the [CD(+)$_{254}$]-**1** enantiomer.

Figure S18: Specific Optical Rotation (SOR) values measured for [CD(+)$_{254}$]-**2** and [CD(−)$_{254}$]-**2** in CH_2Cl_2 (black), $CHCl_3$ (orange), DMSO (blue) and $C_2H_2Cl_4$ (red) at 25 °C. Plot of the SOR (10^{-1} deg cm^2 g^{-1}) values versus λ (nm) for the [CD(+)$_{254}$]-**2** enantiomer.

Figure S19: Specific Optical Rotation (SOR) values measured for [CD(+)$_{254}$]-**3** and [CD(−)$_{254}$]-**3** in CH_2Cl_2 (black), $CHCl_3$ (orange), DMSO (blue) and $C_2H_2Cl_4$ (red) at 25 °C. Plot of the SOR (10^{-1} deg cm^2 g^{-1}) values versus λ (nm) for the [CD(+)$_{254}$]-**3** enantiomer.

Figure S20: ECD spectra of [CD(+)$_{254}$]-**1** (black spectra) and [CD(−)$_{254}$]-**1** (red spectra) recorded in CH_2Cl_2, $CHCl_3$, THF, CH_3CN, DMSO and $C_2H_2Cl_4$ at 20 °C. (c = 10^{-4} – 10^{-5} M). UV-visible spectrum of **1** recorded in THF at 25 °C (c = 1.12 10^{-5} M).

Figure S21: ECD spectra of [CD(+)$_{254}$]-**2** (black spectra) and [CD(−)$_{254}$]-**2** (red spectra) recorded in CH_2Cl_2, $CHCl_3$, THF, CH_3CN, DMSO and $C_2H_2Cl_4$ at 20 °C. (c = 10^{-4} – 10^{-5} M). UV-visible spectrum of **2** recorded in THF at 25 °C (c = 1.02 10^{-5} M).

Figure S22: ECD spectra of [CD(+)$_{254}$]-**3** (black spectra) and [CD(−)$_{254}$]-**3** (red spectra) recorded in CH_2Cl_2, $CHCl_3$, THF, CH_3CN, DMSO and $C_2H_2Cl_4$ at 20 °C. (c = 10^{-4} – 10^{-5} M). UV-visible spectrum of **3** recorded in THF at 25 °C (c = 0.99 10^{-5} M).

Figure S23: IR spectra of a) [CD(+)$_{254}$]-**1**, b) [CD(+)$_{254}$]-**2** and [CD(+)$_{254}$]-**3** c) in $CDCl_3$ (black spectra), CD_2Cl_2 (red spectra) and $C_2D_2Cl_4$ (blue spectra) solvents (0.015 mM, 250 μm path length).

Figure S24: VCD spectra of [CD(+)$_{254}$]-**1** (black spectra) and [CD(−)$_{254}$]-**1** (red spectra) in a) $CDCl_3$, b) CD_2Cl_2, and c) $C_2D_2Cl_4$ solvents (0.015 mM, 250 μm path length).

Figure S25: VCD spectra of [CD(+)$_{254}$]-**2** (black spectra) and [CD(−)$_{254}$]-**2** (red spectra) in a) $CDCl_3$, b) CD_2Cl_2, and c) $C_2D_2Cl_4$ solvents (0.015 mM, 250 μm path length).

Figure S26: VCD spectra of [CD(+)$_{254}$]-**3** (black spectra) and [CD(−)$_{254}$]-**3** (red spectra) in a) CD_2Cl_2 and b) $C_2D_2Cl_4$ solvents (0.015 mM, 250 μm path length).

Figure S27: Optimized geometry of *PP*-**1** enantiomer calculated at the density functional theory (DFT) level using B3LYP functional and 6-31G** basis set with the use of IEFPCM model of solvent (IEFPCM = CH_2Cl_2 and $C_2H_2Cl_4$).

Figure S28: Optimized geometry of *MM*-**2** enantiomer calculated at the density functional theory (DFT) level using B3LYP functional and 6-31G** basis set with the use of IEFPCM model of solvent (IEFPCM = CH_2Cl_2 and $C_2H_2Cl_4$).

Figure S29: Comparison of experimental VCD spectrum of [CD(–)$_{254}$]-**2** in $C_2D_2Cl_4$ solution (15 mM, 250 μm path length) and VCD spectra of *MM*-**2** calculated at the B3LYP/6-31G** level (IEFPCM = $C_2H_2Cl_4$) for the *trans* and *gauche-gauche* conformations of the ethylenedioxy and propylenedioxy linkers, respectively, and for the acetate group grafted on the propylenedioxy linker pointing inside (blue spectrum) or outside (red spectrum) the cavity.

Table S1: Specific optical rotation values measured for [CD(+)$_{254}$]-**1** in different solvents at 25 °C.

Table S2: Specific optical rotation values measured for [CD(–)$_{254}$]-**1** in different solvents at 25 °C.

Table S3: Specific optical rotation values measured for [CD(+)$_{254}$]-**2** in different solvents at 25 °C.

Table S4: Specific optical rotation values measured for [CD(–)$_{254}$]-**2** in different solvents at 25 °C.

Table S5: Specific optical rotation values measured for [CD(+)$_{254}$]-**3** in different solvents at 25 °C.

Table S6: Specific optical rotation values measured for [CD(–)$_{254}$]-**3** in different solvents at 25 °C.

Table S7: B3LYP/6-31G** frequencies (scaled by 0.968) of the ester νC=O stretching vibration of *MM*-**2** (IEFPCM = CH_2Cl_2 and $C_2D_2Cl_4$) for the acetate group pointing inward or outward the cavity.

Analytical separation for compound **1**

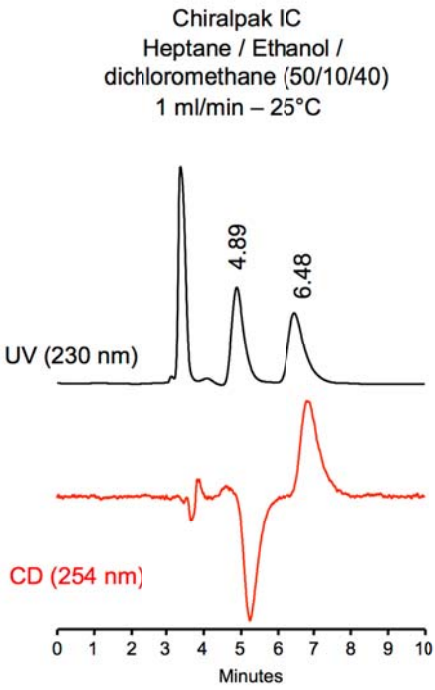

Column	Mobile Phase	t_1	k_1	t_2	k_2	α	Rs
Chiralpak IC	heptane/EtOH/CH_2Cl_2 (50/10/40)	4.89 (-)	0.63	6.48 (+)	1.16	1.84	2.23

Figure S1: Chromatograms (Chiralpak IC, 250 x 4.6 mm, heptane/ethanol/CH_2Cl_2: 50/10/40, 1 mL/min at 25 °C) of the (rac)-**1** before preparative separation on Chiralpak IC (250 x 10 mm, heptane/ethanol/CH_2Cl_2: 50/10/40, 5 mL/min).

Semi-preparative separation for compound **1**

Sample preparation: About 460 mg of compound (rac)-**1** are dissolved in 18 mL of dichloromethane. Chromatographic conditions: Chiralpak IC (250 x 10 mm), hexane/ethanol/dichloromethane (5/1/4) as mobile phase, flow-rate = 5 ml/min, UV detection at 230 nm. Injections (stacked): 180 times 100 µL, every 5 minutes.
The first eluted enantiomer is collected between 4.2 and 5.2 minutes and the second one between 6 and 7.5 minutes.
First fraction: 180 mg of the first eluted [CD(–)$_{254}$]-**1** with ee > 99.5 % on Jasco CD-1595 circular dichroism detector at 254 nm.
Second fraction: 200 mg of the second eluted [CD(+)$_{254}$]-**1** with ee > 99 % on Jasco CD-1595 circular dichroism detector at 254 nm.

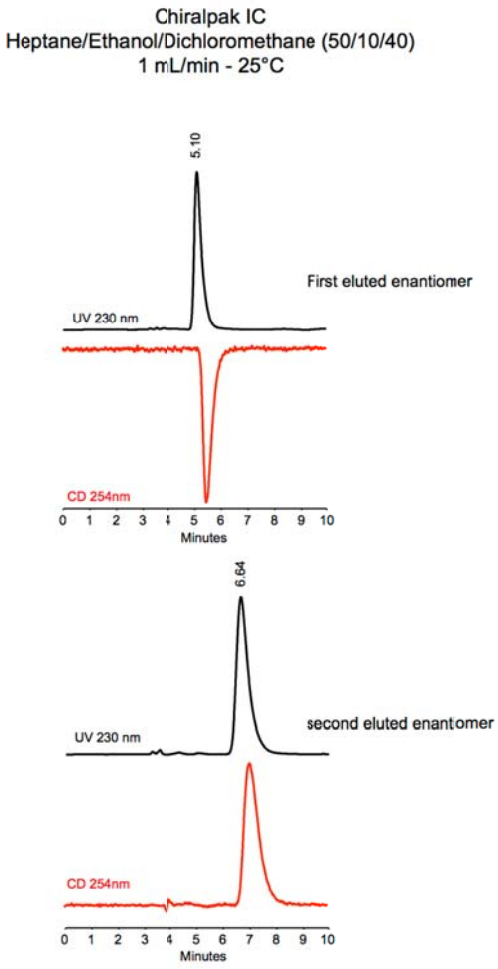

Figure S2: Chromatograms (Chiralpak IC, 250 x 4.6 mm, heptane/ethanol/CH_2Cl_2: 50/10/40, 1 mL/min at 25 °C) of the collected [CD(–)$_{254}$]-**1** and [CD(+)$_{254}$]-**1** after preparative separation on Chiralpak IC (250 x 10 mm, heptane/ethanol/CH_2Cl_2: 50/10/40, 5 mL/min). Detection performed by UV-Vis spectroscopy at 230 nm (black chromatograms) and CD spectroscopy at 254 nm (red chromatograms).

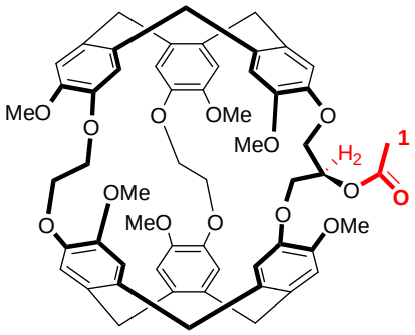

Synthesis of cryptophane 2: Acetic anhydride (0.7 mL, 7.4 mmol, 10 equiv.) was added dropwise at 0 °C to a solution of cryptophane-223$(OMe)_6OH$ (0.7 g, 0.75 mmol) in freshly distilled CH_2Cl_2 (23 mL) and pyridine (3.5 mL). The reaction mixture was stirred for 48 hours at room temperature. The solution was then quenched at 0 °C with concentrated $NaHCO_3$ (10 ml) for 10 minutes and then poured in 20 mL of H_2O. The aqueous layer was extracted 5 times with CH_2Cl_2 and then dried over Na_2SO_4. After filtration the solvent was evaporated under reduced pressure. The crude product was subjected to column chromatography on silica gel (CH_2Cl_2/acetone: 85/15) to give rise to compound **2** as a white product (0.52 g, 71%). ^{1}H NMR (300 MHz, $CDCl_3$, 25 °C) δ ppm: 6.63-6.79 (12 s, 12 H), 4.58-4.62 (m, 6H), 4.02-4.2 (m, 11H), 3.93 (m, 1 H), 3.73- 3.8 (6s, 18 H), 3.47 (m, 1H), 3.36-3.41 (m, 6 H), 2.17 (s, 3H). ^{13}C NMR: (75.5 MHz, $CDCl_3$, 25 °C) δ ppm: 170.6, 149.6 (2C), 149.55, 149.4, 148.8, 148.1, 146.8, 146.7 (2 C), 146.6, 146.5 (2 C), 134.1, 134.1, 133.8, 133.8, 133.3, 132.8, 132.1, 131.9, 131.5, 131.4, 131.35, 131.3, 120.3, 120.2 (3 C), 117.2, 115.1, 114.2 (2 C), 113.9, 113.7, 113.35, 113.2, 70.8, 69.6, 69.5, 69.1, 68.9 (2 C), 66.6, 56.3, 56.3, 55.7, 55.65(2 C), 55.6, 36.5, 36.4; 36.2 (4 C), 21.2. HRMS(ESI-TOF) *m/z* $[M + Na]^+$ calcd for $C_{57}H_{58}O_{14}Na$ 989.3724, found 989.3719.

Figure S3: Experimental procedure for the synthesis of cryptophane **2**.

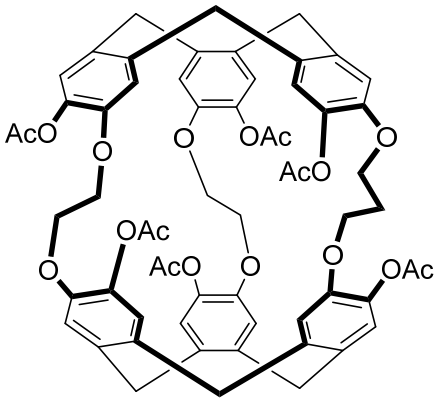

Synthesis of cryptophane 3: Acetic anhydride (2.2 mL, 41 mmol) was added dropwise at 0 °C to a solution of cryptophane223$(OH)_6$ (0.35g, 0.42 mmol) in Pyridine (5 mL). The reaction was stirred at room temperature for 16 hours under an argon atmosphere. Then, the reaction was quenched with a solution of sodium bicarbonate at 0 °C. The solution was then extracted 5 times with CH_2Cl_2. The combined organic layers were dried over sodium sulfate. A filtration, followed by evaporation of the solvents under reduced pressure, gives rise to compound **3** as a white product. The solid was then washed on a frit with an Et_2O/CH_2Cl_2: 75/25 mixture to give compound **3** as a clean white solid (0.31g, 71 %). ^{1}H NMR (300 MHz, $CDCl_3$, 25 °C) δ ppm: 6.94 (s, 2 H), 6.91(2 H), 6.89 (2 H), 6.87 (2 H), 6.86(2 H), 6.62 (2 H), 4.65-4.58 (m, 6 H), 4.28-4.286 (2 H, m), 4.16-4.15 (m, 2 H), 4.04 - 3.8 (m, 8 H), 3.5-3.4 (m, 6H), 2.31 (s, 6 H), 2.29 (s, 6 H), 2.25 (s, 6 H), 2.09 (m, 2 H). ^{13}C NMR (75.5 MHz, $CDCl_3$, 25 °C) δ ppm: 168.5 (4 C), 168.3 (2 C), 149.3 (2 C), 149.25 (2 C), 149.0 (2 C), 140.5 (2 C), 140.3 (2 C), 138.7 (2 C), 138.6 (2 C), 137.8 (2 C), 136.7 (2 C), 133.6 (2 C), 133.4 (2 C), 131.2 (2 C), 124.4 (2 C), 124.0 (2 C), 123.3 (2 C), 120.9 (2 C), 120.7 (2 C), 113.6 (2 C), 69.8 (2 C), 69.1 (2 C), 63.7 (2 C), 36.4 (2 C), 36.1 (4 C), 20.7 (4 C), 20.6 (2 C). HRMS(ESI-TOF) *m/z* $[M + Na]^+$ calcd for $C_{61}H_{56}O_{18}Na$ 1099.3364, found 1099.3359.

Figure S4: Experimental procedure for the synthesis of cryptophane **3**.

Analytical separation for compound **2**

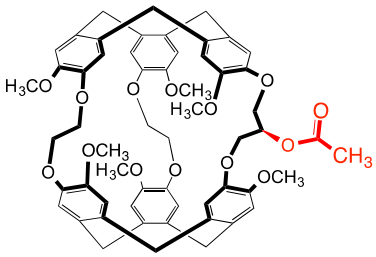

(S,S)-Whelk-O_1
Heptane/ethanol/CH_2Cl_2
(20/40/40)
1 ml/min – 25°C

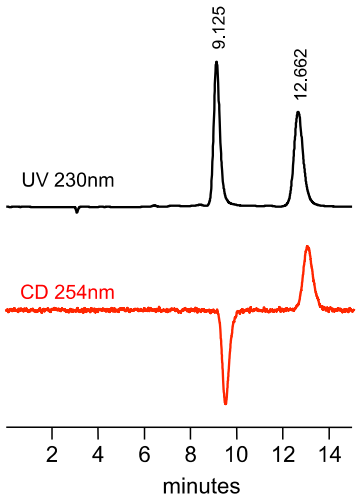

Column	Mobile Phase	t_1	k_1	t_2	k_2	α	Rs
(*S*,*S*)-Whelk-O_1	heptane/EtOH/CH_2Cl_2 20/40/40	9.13 (-)	2.10	12.67 (+)	3.29	1.57	5.72

Figure S5: Chromatograms ((*S*,*S*)-Whelk-O_1, 250 x 4.6 mm, heptane/ethanol/CH_2Cl_2: 20/40/40, 1 mL/min at 25 °C) of the (rac)-**2** before preparative separation on (*S*,*S*)-Whelk-O_1 (250 x 10 mm, heptane/ethanol/CH_2Cl_2: 20/40/40, 5 mL/min).

Semi-preparative separation for compound **2**

Sample preparation: About 580 mg of (rac)-**2** are dissolved in 6 mL of dichloromethane. Chromatographic conditions: (*S*,*S*)-Whelk-O1 (250 x 10 mm), heptane/ethanol/ dichloromethane (20/40/40) as mobile phase, flow-rate = 5 mL/min, UV detection at 230 nm. Injections (stacked): 20 times 300 µL, every 13.8 minutes.
First fraction: 255 mg of the first eluted [CD(−)$_{254}$]-**2** with ee > 99.5% on Jasco CD-1595 circular dichroism detector at 254 nm.
Second fraction: 240 mg of the second eluted [CD(+)$_{254}$]-**2** with ee > 99.5% on Jasco CD-1595 circular dichroism detector at 254 nm.

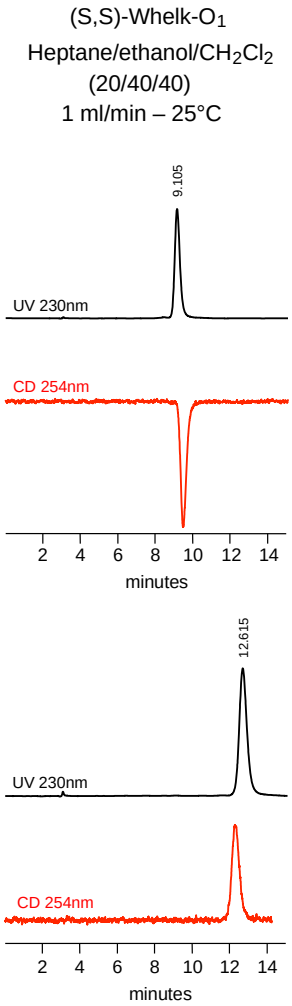

Figure S6: Chromatograms ((*S*,*S*)-Whelk-O$_1$, 250 x 4.6 mm, heptane/ethanol/CH_2Cl_2: 20/40/40, 1 mL/min at 25 °C) of the collected [CD(−)$_{254}$]-**2** and [CD(+)$_{254}$]-**2** after preparative separation on (*S*,*S*)-Whelk-O$_1$ (250 x 10 mm, heptane/ethanol/CH_2Cl_2: 20/40/40, 5 mL/min). Detection performed by UV-Vis spectroscopy at 230 nm (black chromatograms) and CD spectroscopy at 254 nm (red chromatograms).

Analytical separation for compound **3**

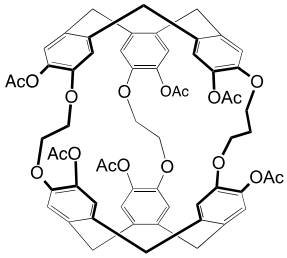

(S,S)-Whelk-O1
Ethanol/CH_2Cl_2
(50/50)
1 ml/min – 25°C

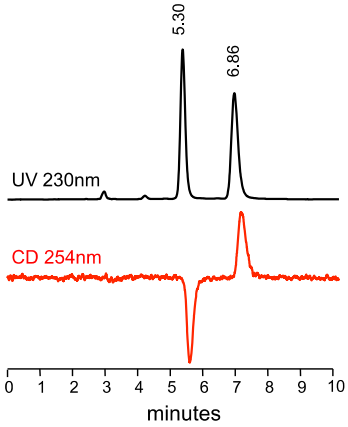

Column	Mobile Phase	t_1	k_1	t_2	k_2	α	Rs
(*S*,*S*)-Whelk-O1	ethanol/CH_2Cl_2 50/50	5.30 (-)	0.80	6.86 (+)	1.32	1.67	4.81

Figure S7: Chromatograms ((*S*,*S*)-Whelk-O_1, 250 x 4.6 mm, ethanol/CH_2Cl_2: 50/50, 1 mL/min at 25 °C) of the (rac)-**3** before preparative separation on (*S*,*S*)-Whelk-O_1 (250 x 10 mm, heptane/ethanol/CH_2Cl_2: 35/65, 5 mL/min).

Semi-preparative separation for compound **3**

Sample preparation: About 575 mg of compound (rac)-**3** are dissolved in 170 mL of a mixture of ethanol/dichloromethane (30/70). Chromatographic conditions: (*S*,*S*)-Whelk-O_1 (250 x 10 mm), ethanol/dichloromethane (35/65) as mobile phase, flow-rate = 5 ml/min, UV detection at 230 nm. Injections (stacked): 340 times 500 µL, every 4.4 minutes.
First fraction: 235 mg of the first eluted [CD(−)$_{254}$]-**3** with ee > 99% on Jasco CD-1595 circular dichroism detector at 254 nm.
Second fraction: 200 mg of the second eluted [CD(+)$_{254}$]-**3** with ee > 99.5% on Jasco CD-1595 circular dichroism detector at 254 nm.

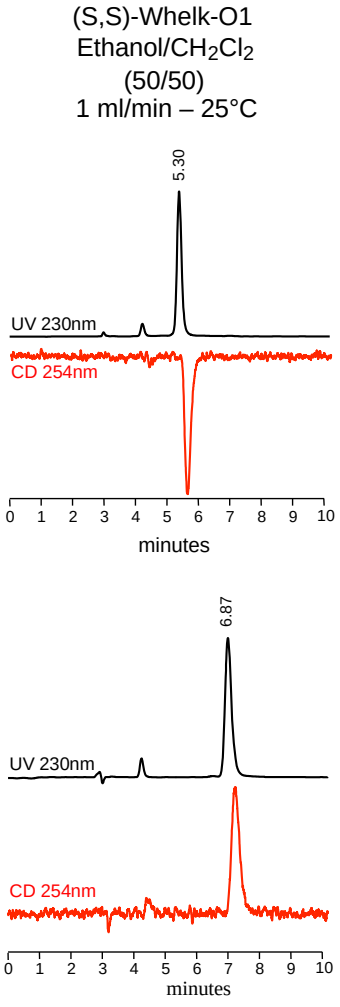

Figure S8: Chromatograms ((*S*,*S*)-Whelk-O_1, 250 x 4.6 mm, ethanol/CH_2Cl_2: 50/50, 1 mL/min at 25 °C) of the collected [CD(−)$_{254}$]-**3** and [CD(+)$_{254}$]-**3** after preparative separation on (*S*,*S*)-Whelk-O_1 (250 x 10 mm, ethanol/CH_2Cl_2: 50/50, 5 mL/min). Detection performed by UV-Vis spectroscopy at 230 nm (black chromatograms) and CD spectroscopy at 254 nm (red chromatograms).

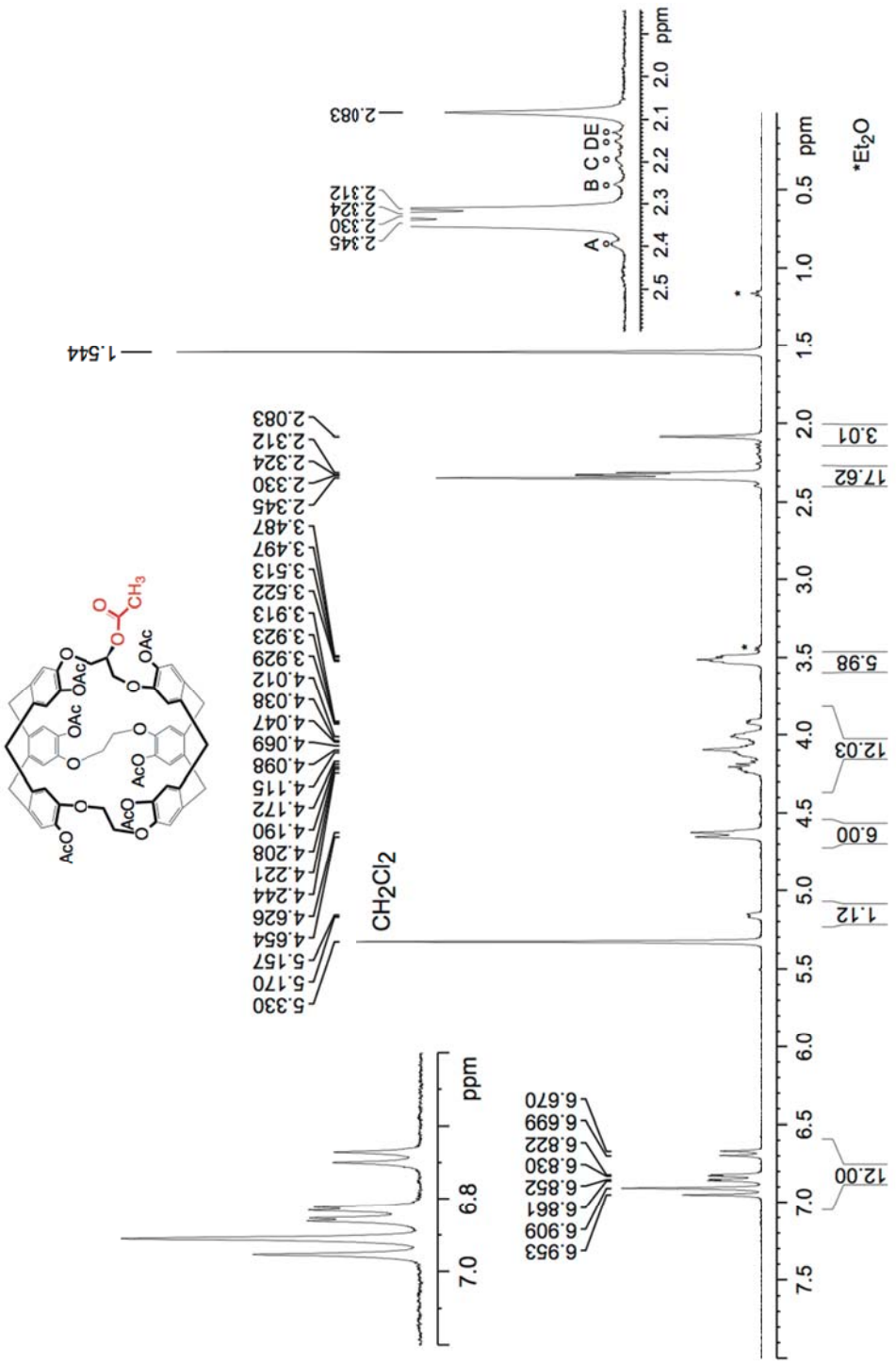

Figure S9: ^{1}H NMR spectrum (300 MHz) of (rac)-**1** recorded in CD_2Cl_2 at 25 °C. The letters A,B,C,D,E show protons signals related to the imploded form.

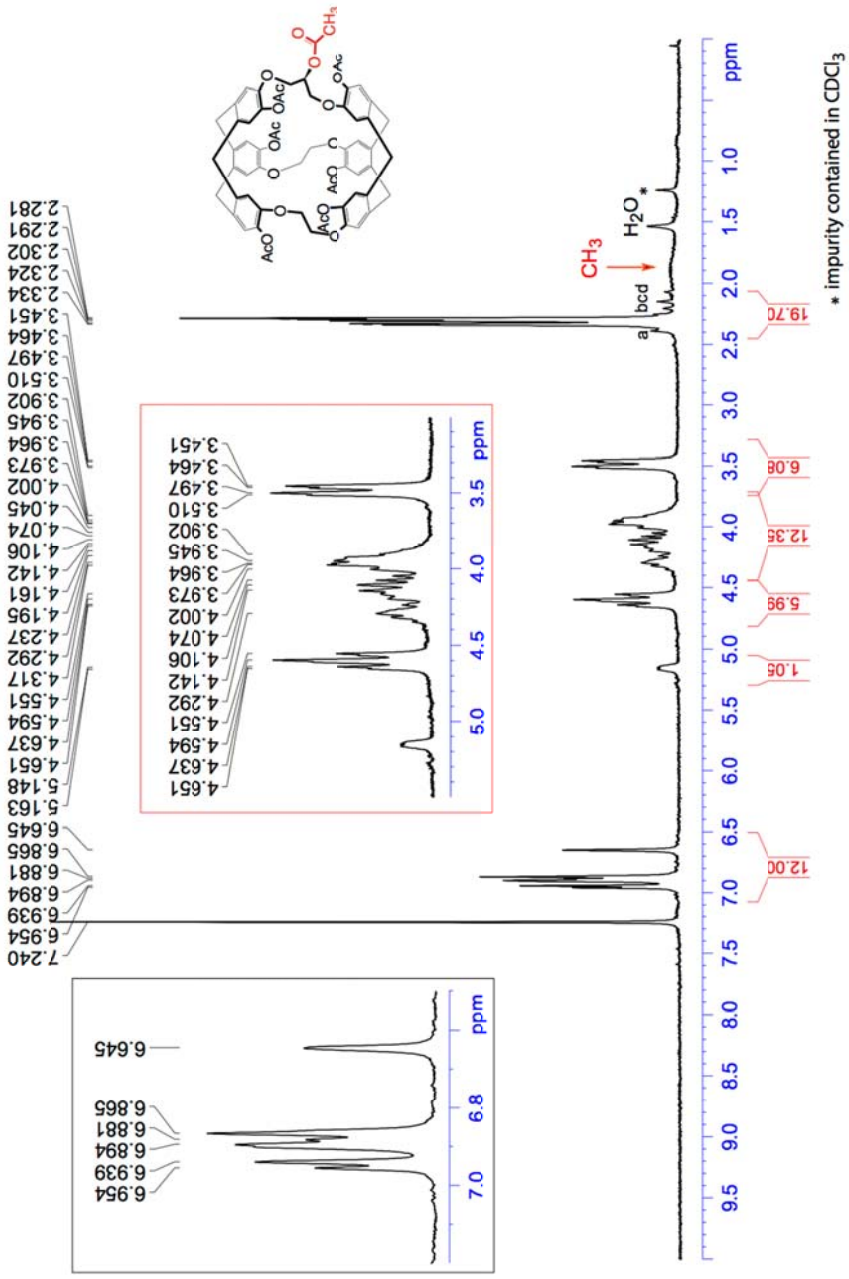

Figure S10: ^{1}H NMR spectrum (300 MHz) of (rac)-**1** recorded in $CDCl_3$ at 25 °C. The letters A,B,C,D show protons signals related to the imploded form.

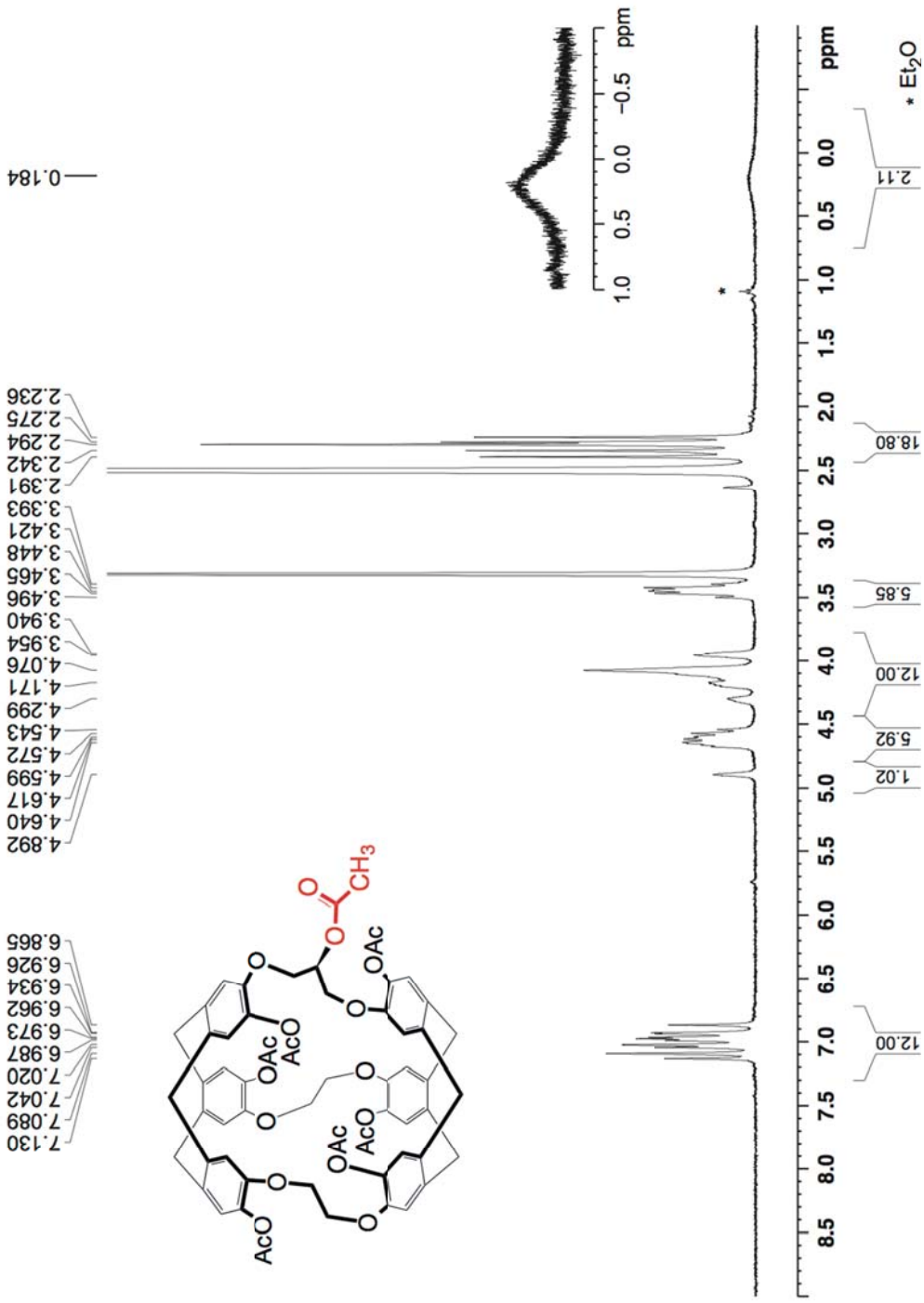

Figure S11: ^{1}H NMR spectrum (300 MHz) of (rac)-**1** recorded in DMSO-d_6 at 25 °C.

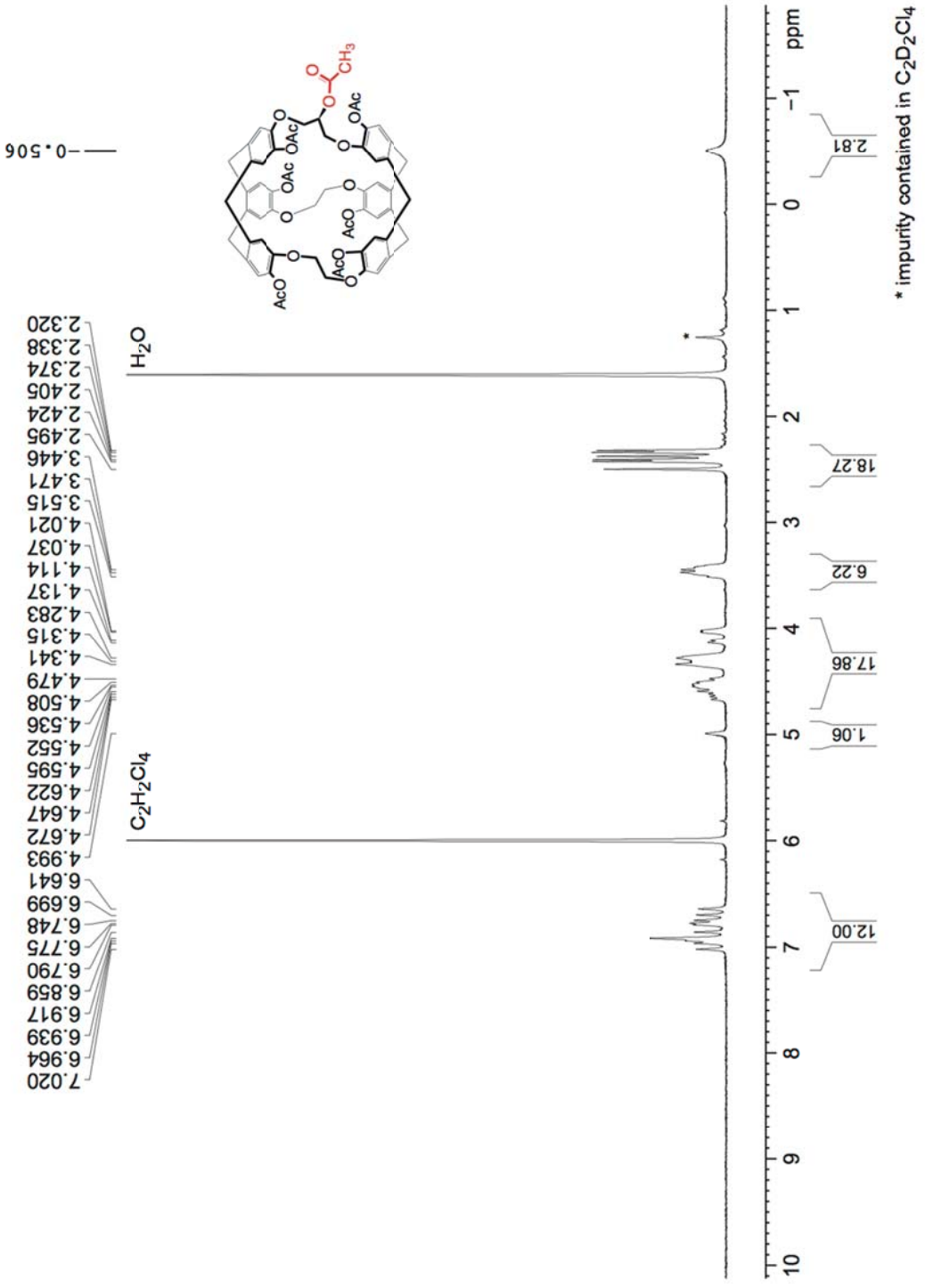

Figure S12: ^{1}H NMR spectrum (300 MHz) of (rac)-**1** recorded in 1,1,2,2-tetrachloroethane-d_2 at 25 °C.

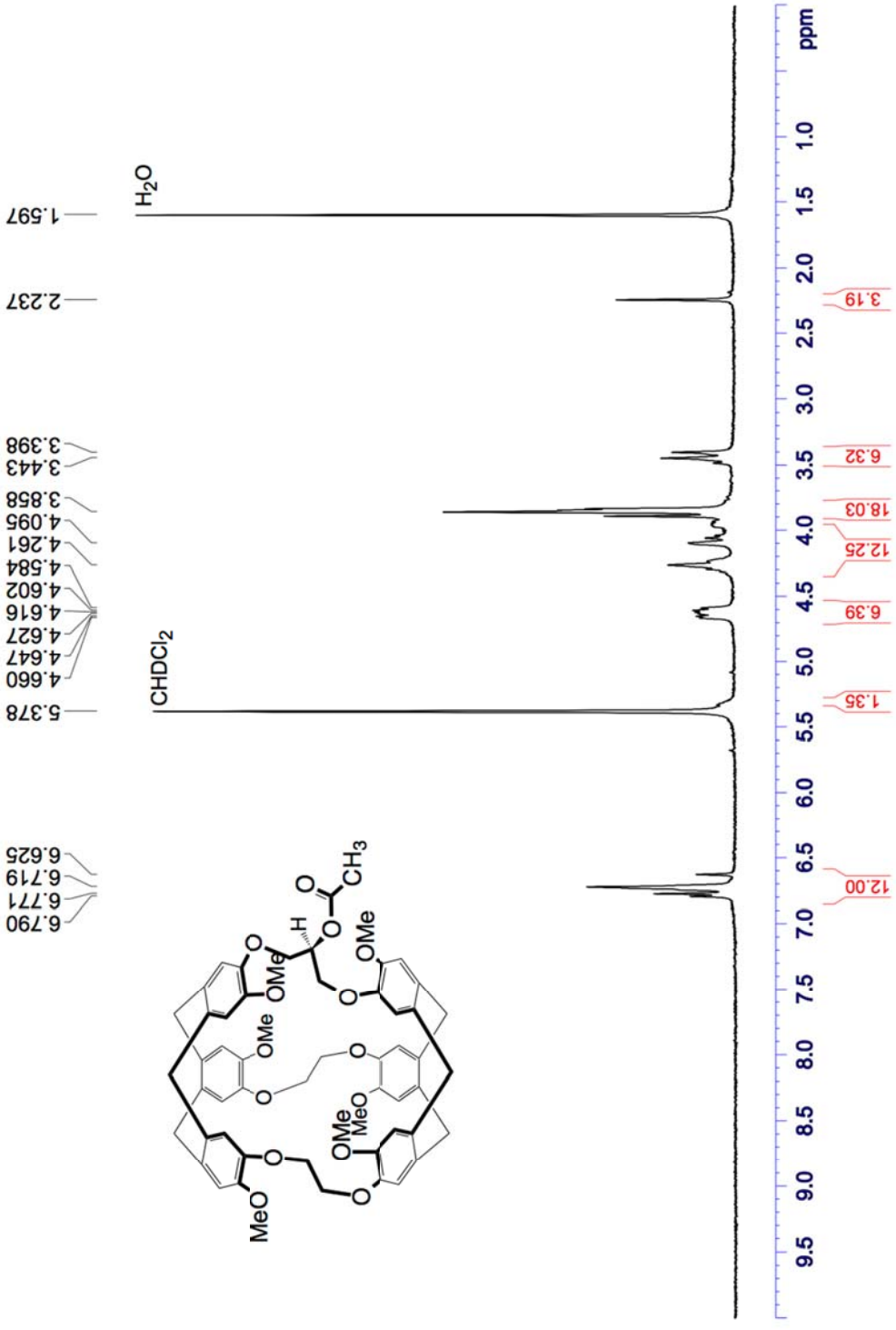

Figure S13: ^{1}H NMR spectrum (300 MHz) of (rac)-**2** recorded in CD_2Cl_2 at 25 °C.

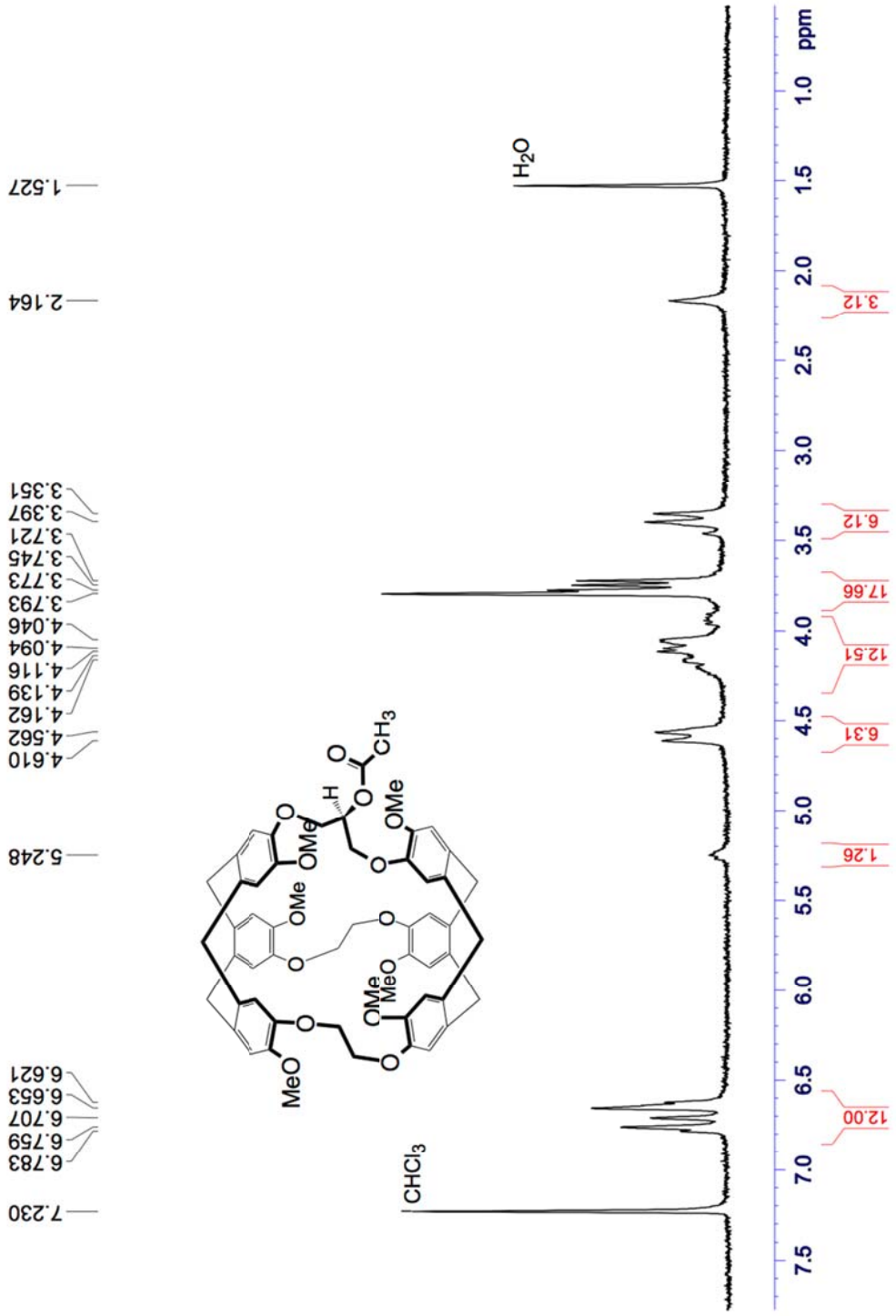

Figure S14: ^{1}H NMR spectrum (300 MHz) of (rac)-**2** recorded in $CDCl_3$ at 25 °C.

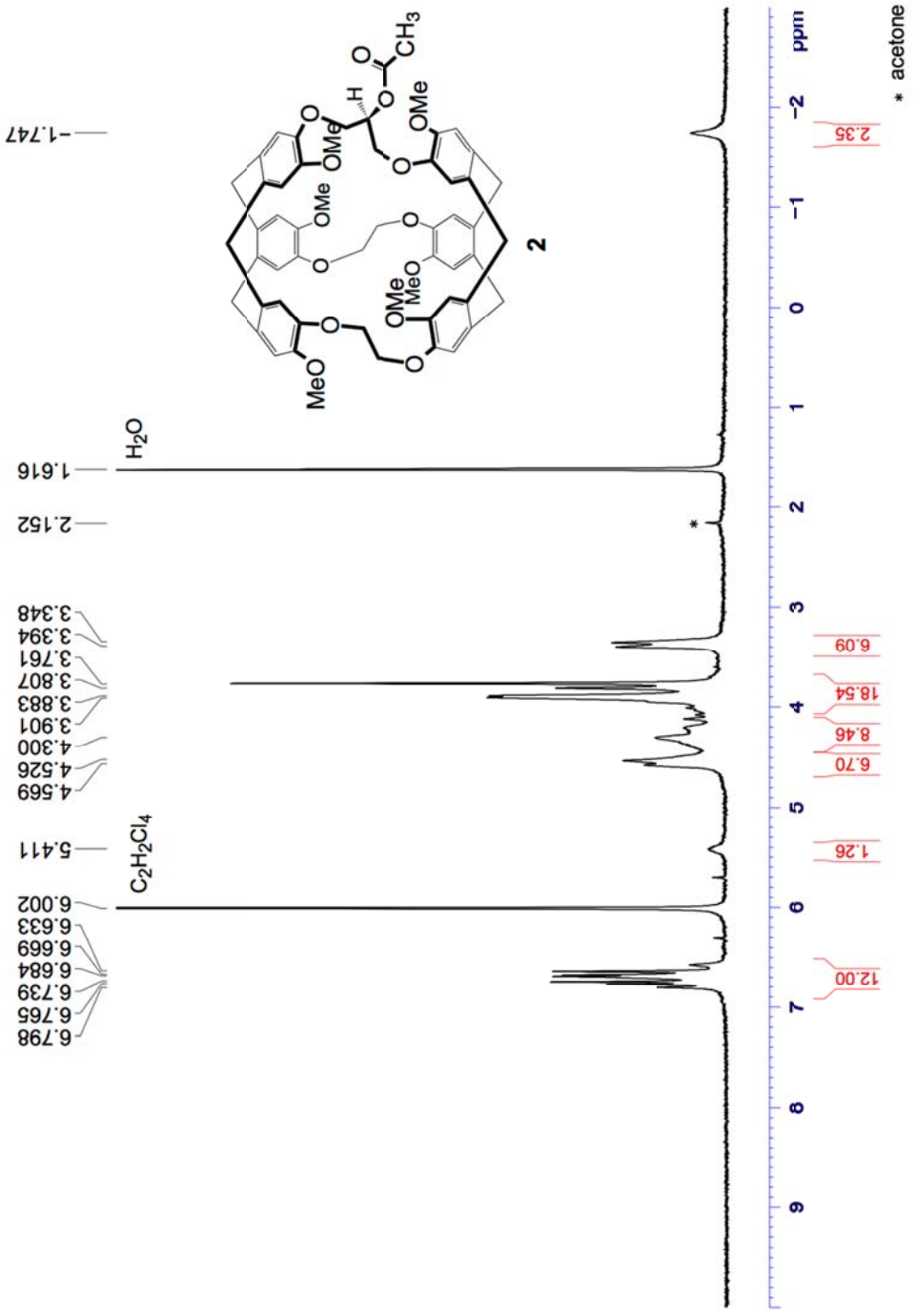

Figure S15: ^{1}H NMR spectrum (300 MHz) of (rac)-**2** recorded in 1,1,2,2-tetrachloroethane-d_2 at 25 °C.

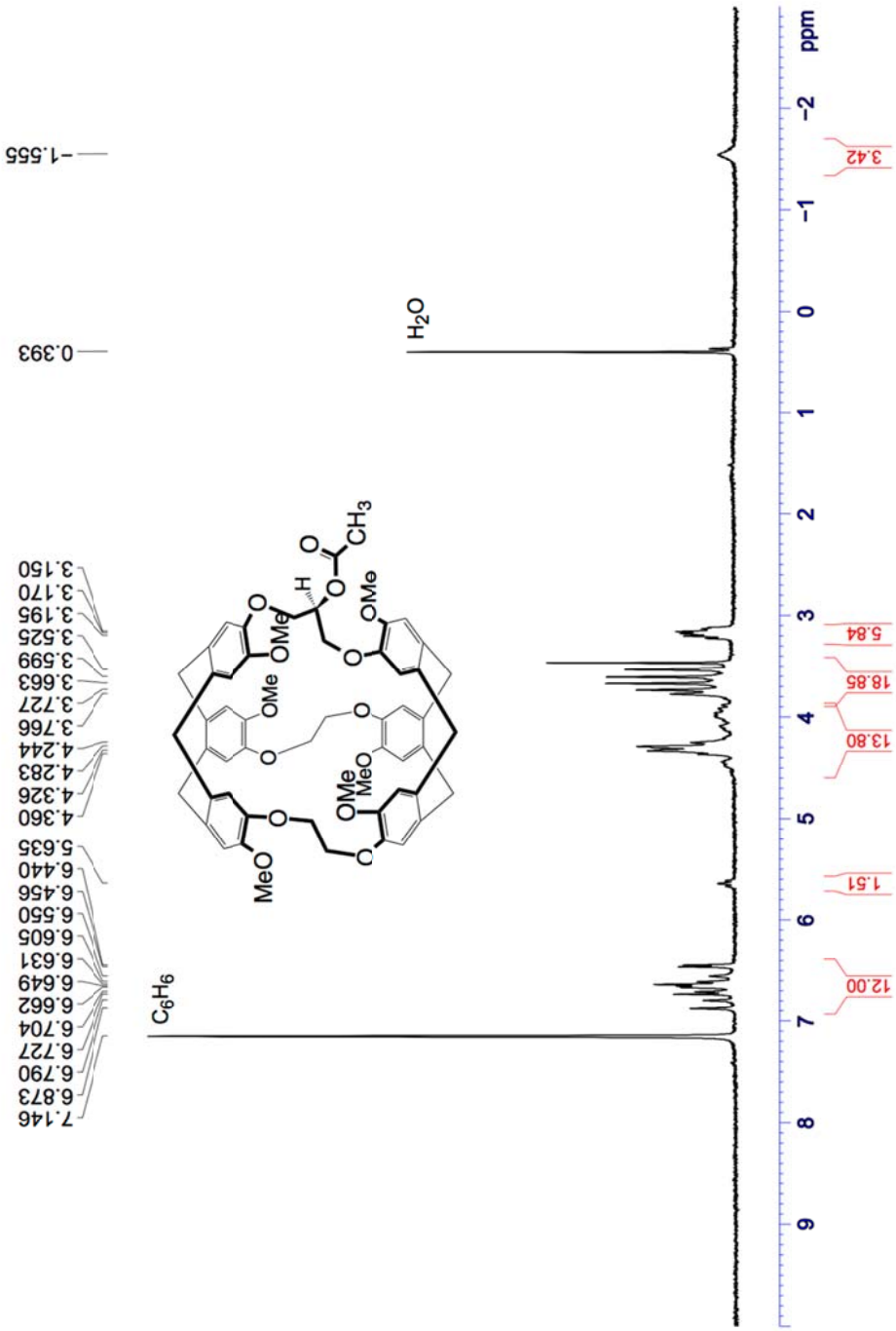

Figure S16: ^{1}H NMR spectrum (300 MHz) of (rac)-**2** recorded in benzene-d_6 at 25 °C.

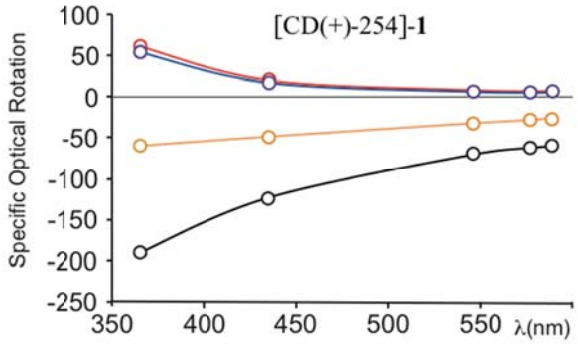

Figure S17: Specific Optical Rotation (SOR) values measured for [CD(+)$_{254}$]-**1** and [CD(–)$_{254}$]-**1** in CH_2Cl_2 (black), $CHCl_3$ (orange), DMSO (blue) and $C_2H_2Cl_4$ (red) at 25 °C. Plot of the SOR (10^{-1} deg cm^2 g^{-1}) values versus λ (nm) for the [CD(+)$_{254}$]-**1** enantiomer.

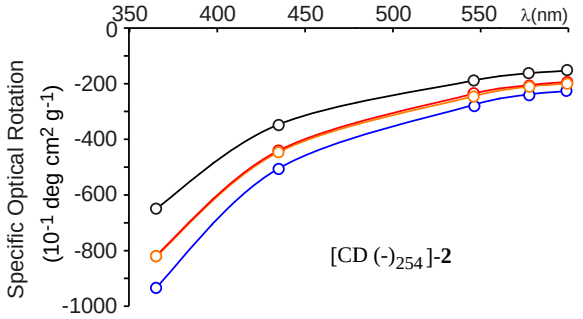

Figure S18: Specific Optical Rotation (SOR) values measured for [CD(+)$_{254}$]-**2** and [CD(–)$_{254}$]-**2** in CH_2Cl_2 (black), $CHCl_3$ (orange), DMSO (blue) and $C_2H_2Cl_4$ (red) at 25 °C. Plot of the SOR (10^{-1} deg cm^2 g^{-1}) values versus λ (nm) for the [CD(+)$_{254}$]-**2** enantiomer.

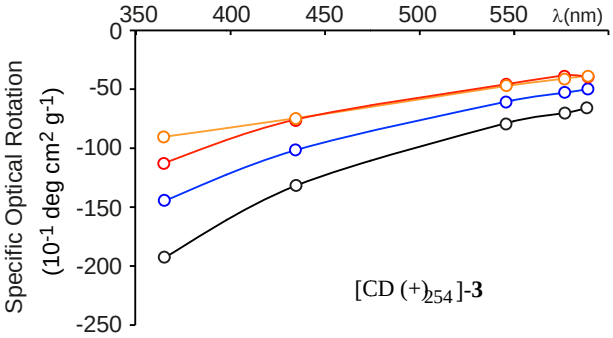

Figure S19: Specific Optical Rotation (SOR) values measured for [CD(+)$_{254}$]-**3** and [CD(–)$_{254}$]-**3** in CH_2Cl_2 (black), $CHCl_3$ (orange), DMSO (blue) and $C_2H_2Cl_4$ (red) at 25 °C. Plot of the SOR (10^{-1} deg cm^2 g^{-1}) values versus λ (nm) for the [CD(+)$_{254}$]-**3** enantiomer.

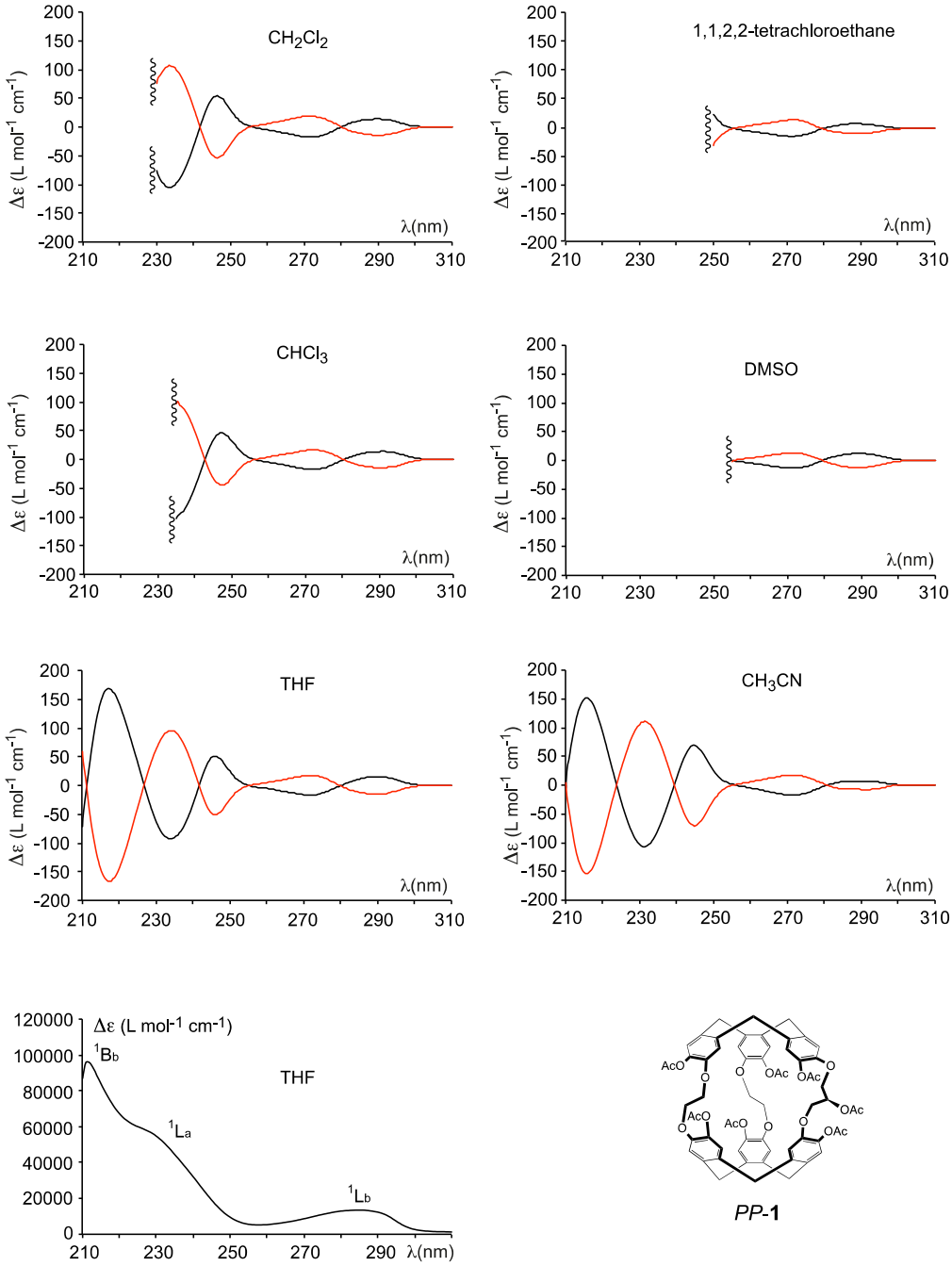

Figure S20: ECD spectra of [CD(+)$_{254}$]-**1** (black spectra) and [CD(−)$_{254}$]-**1** (red spectra) recorded in CH_2Cl_2, $CHCl_3$, THF, CH_3CN, DMSO and $C_2H_2Cl_4$ at 20 °C. (c = 10^{-4} – 10^{-5} M). UV-visible spectrum of **1** recorded in THF at 25 °C (c = 1.12 10^{-5} M).

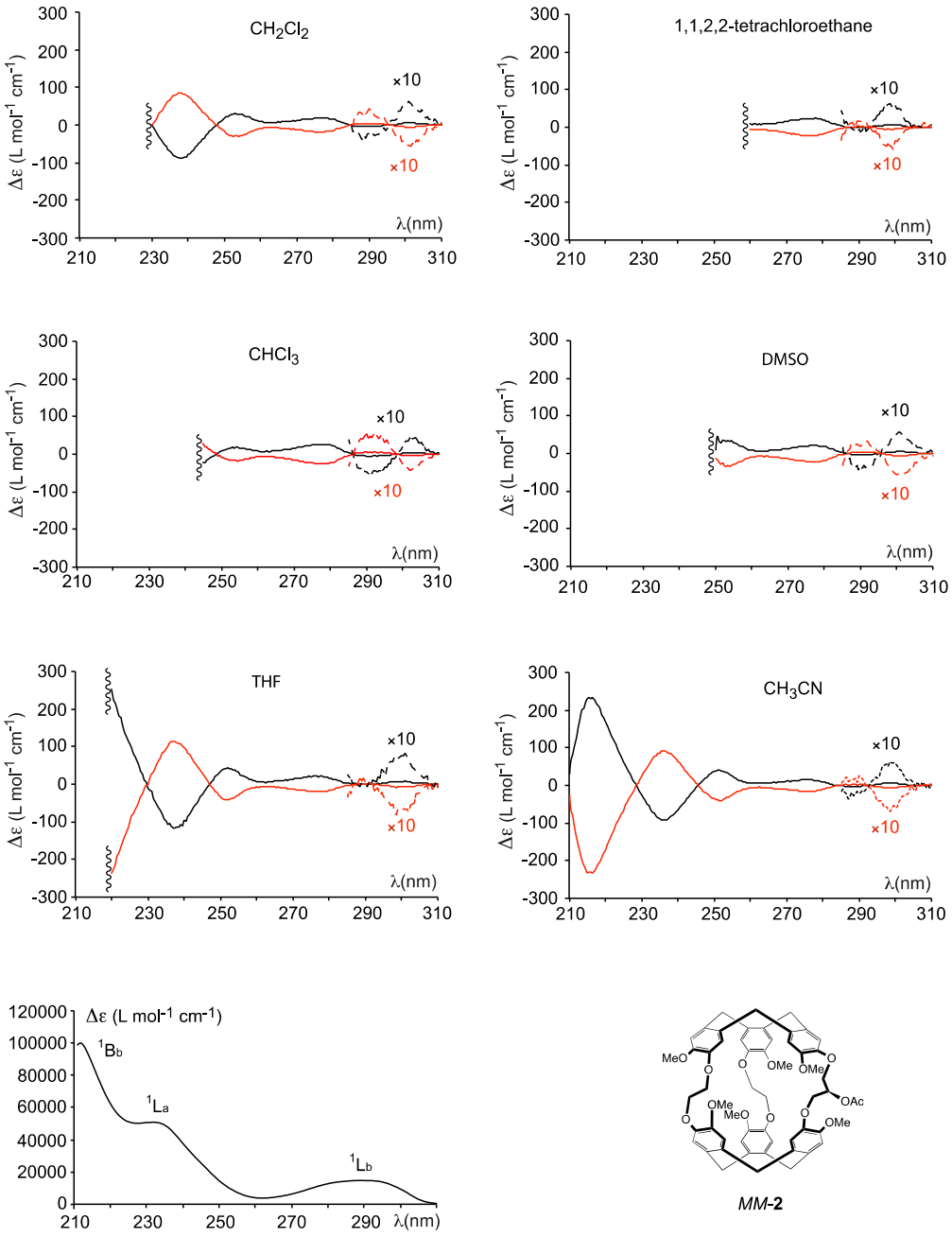

Figure S21: ECD spectra of [CD(+)$_{254}$]-**2** (black spectra) and [CD(–)$_{254}$]-**2** (red spectra) recorded in CH_2Cl_2, $CHCl_3$, THF, CH_3CN, DMSO and $C_2H_2Cl_4$ at 20 °C. (c = 10^{-4} – 10^{-5} M). UV-visible spectrum of **2** recorded in THF at 25 °C (c = 1.02 10^{-5} M).

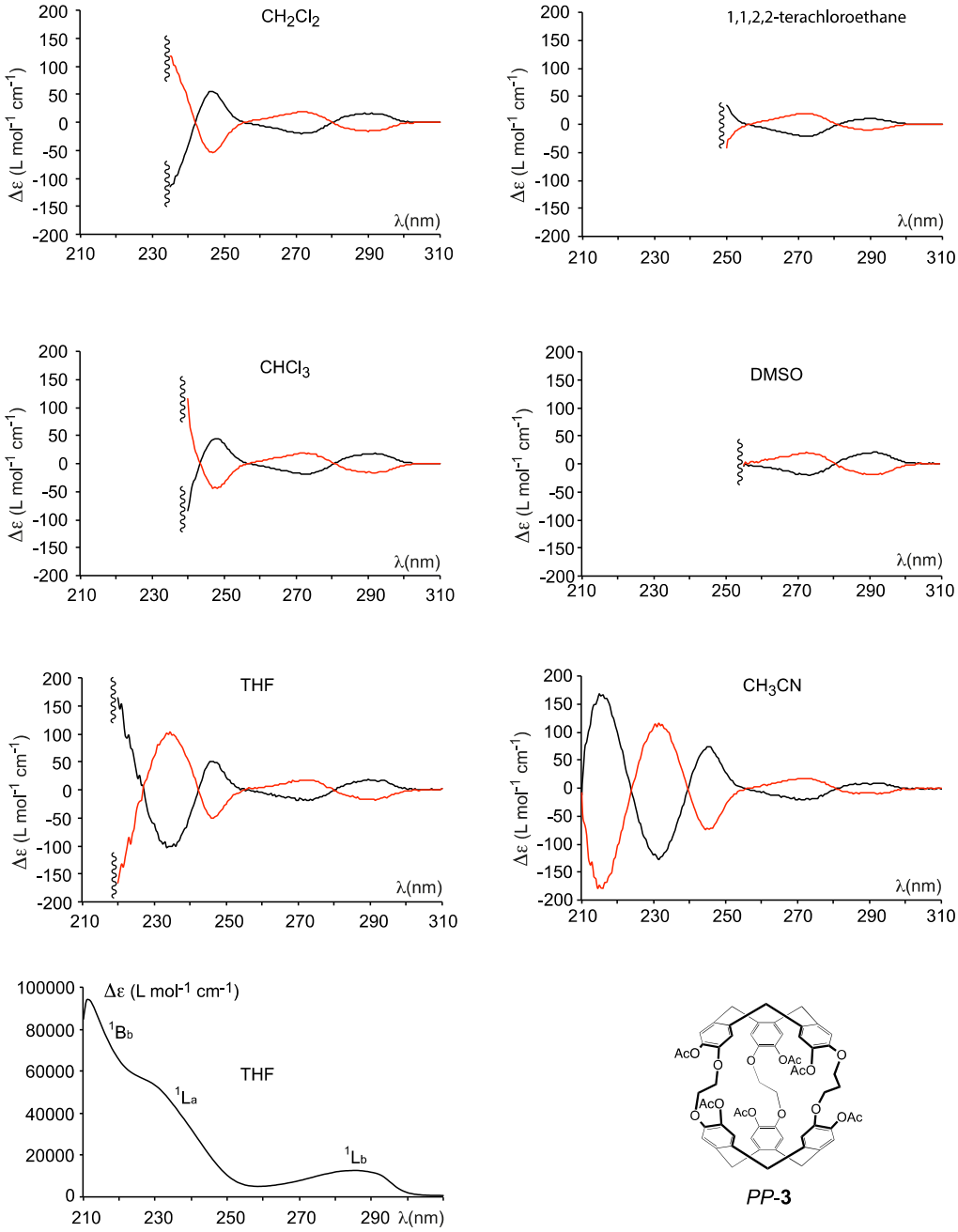

PP-**3**

Figure S22: ECD spectra of [CD(+)$_{254}$]-**3** (black spectra) and [CD(−)$_{254}$]-**3** (red spectra) recorded in CH_2Cl_2, $CHCl_3$, THF, CH_3CN, DMSO and $C_2H_2Cl_4$ at 20 °C. (c = 10^{-4} – 10^{-5} M). UV-visible spectrum of **3** recorded in THF at 25 °C (c = 0.99 10^{-5} M).

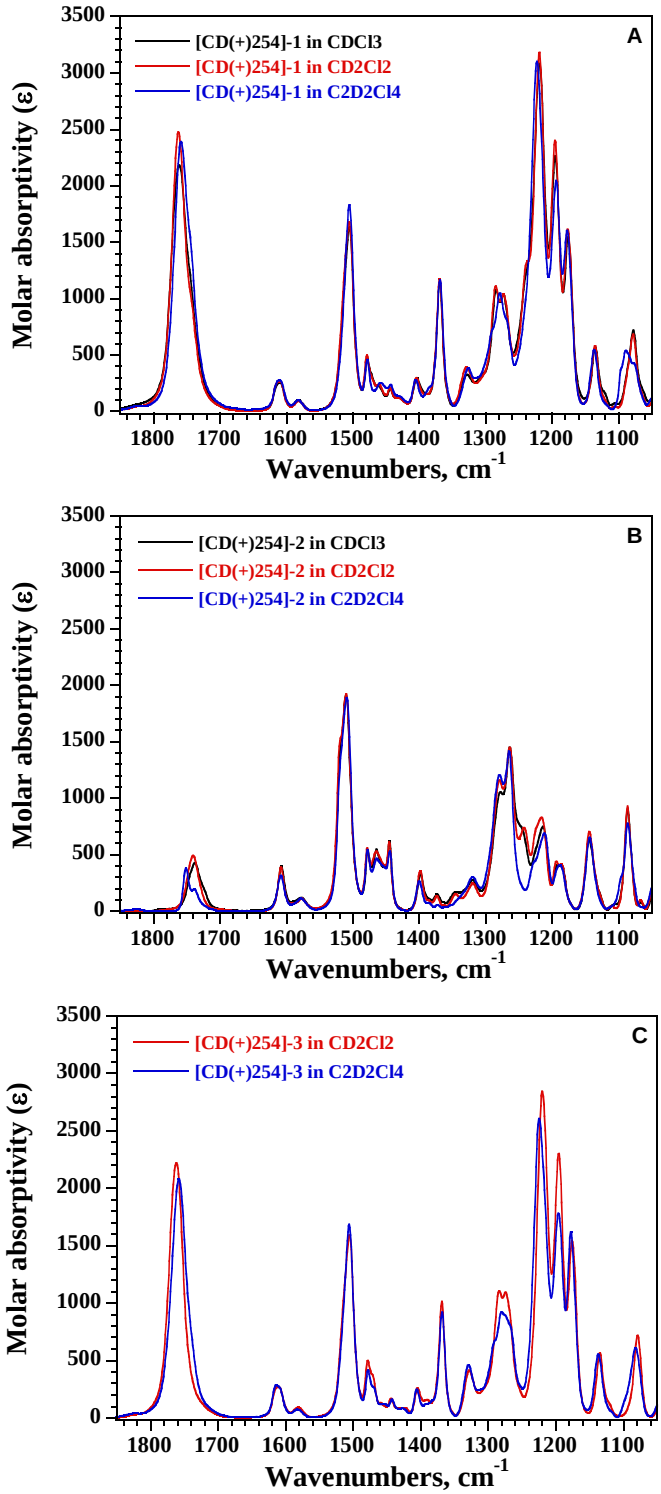

Figure S23: IR spectra of a) [CD(+)$_{254}$]-**1**, b) [CD(+)$_{254}$]-**2** and [CD(+)$_{254}$]-**3** c) in $CDCl_3$ (black spectra), CD_2Cl_2 (red spectra) and $C_2D_2Cl_4$ (blue spectra) solvents (0.015 mM, 250 μm path length).

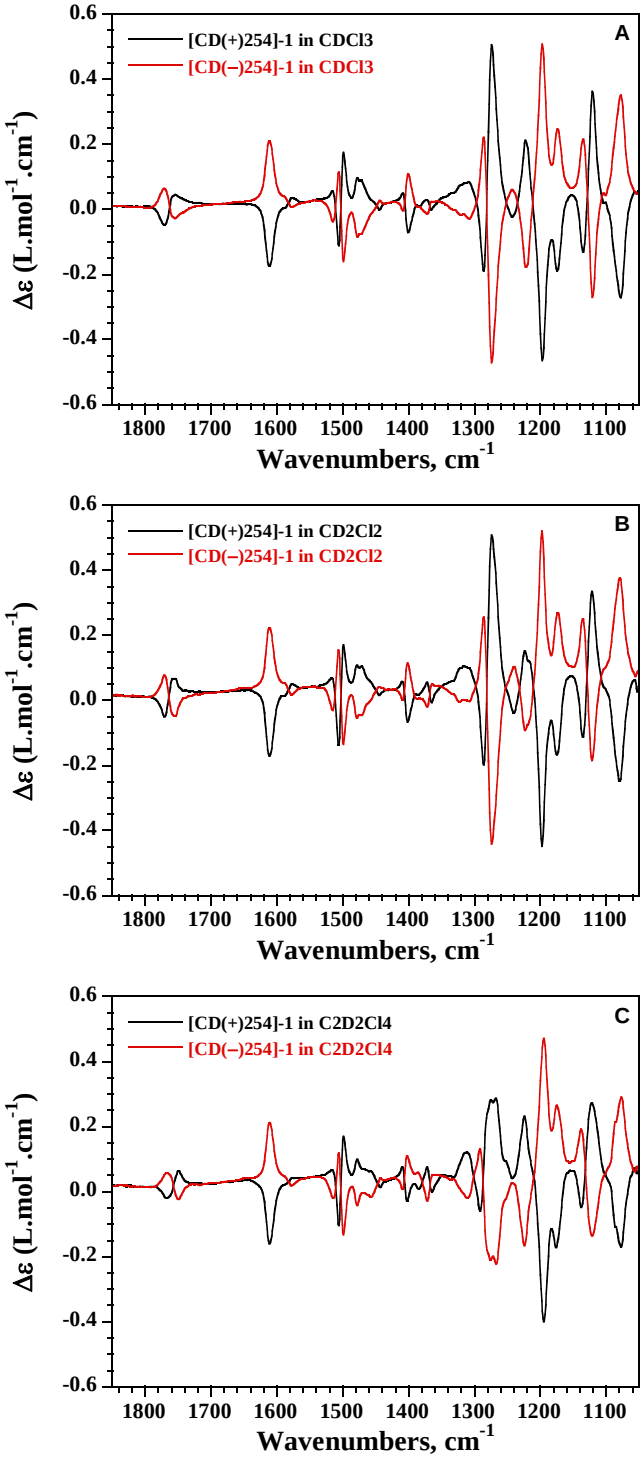

Figure S24: VCD spectra of [CD(+)$_{254}$]-**1** (black spectra) and [CD(–)$_{254}$]-**1** (red spectra) in a) $CDCl_3$, b) CD_2Cl_2, and c) $C_2D_2Cl_4$ solvents (0.015 mM, 250 μm path length).

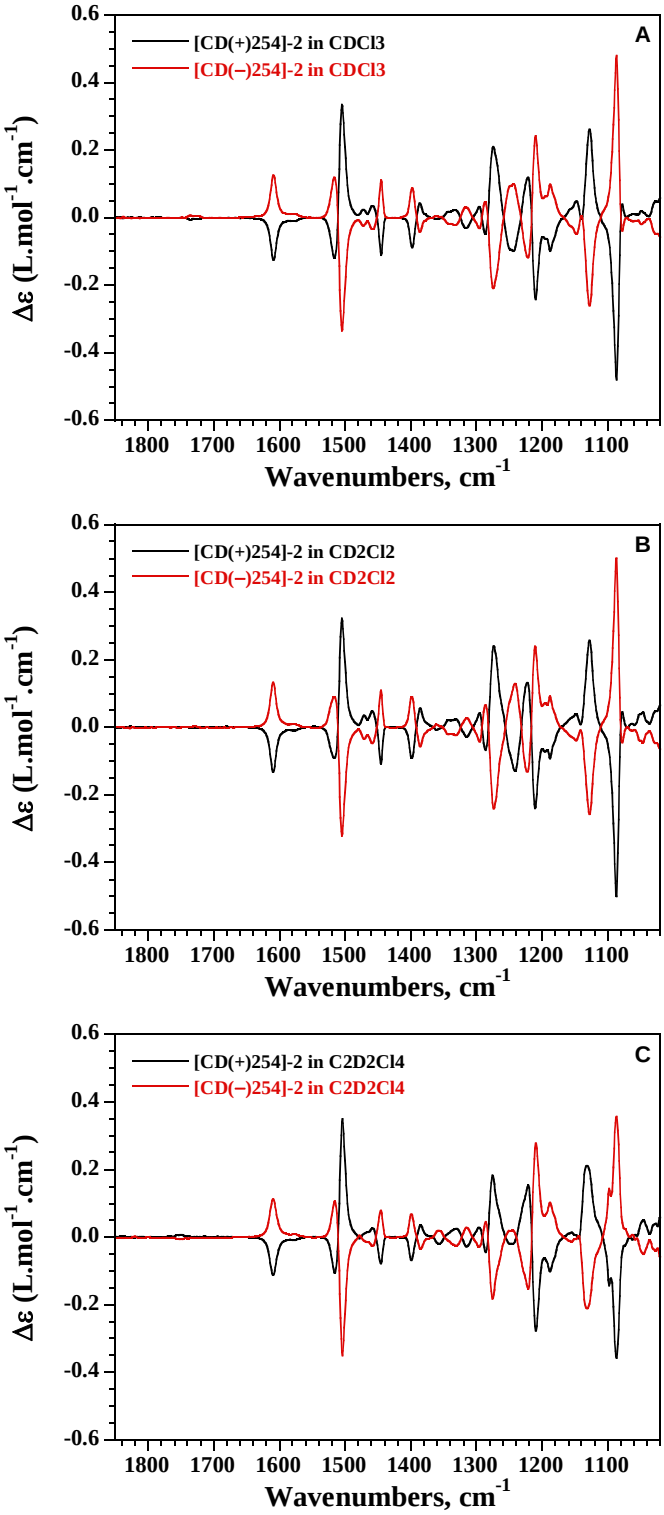

Figure S25: VCD spectra of [CD(+)$_{254}$]-**2** (black spectra) and [CD(−)$_{254}$]-**2** (red spectra) in a) $CDCl_3$, b) CD_2Cl_2, and c) $C_2D_2Cl_4$ solvents (0.015 mM, 250 μm path length).

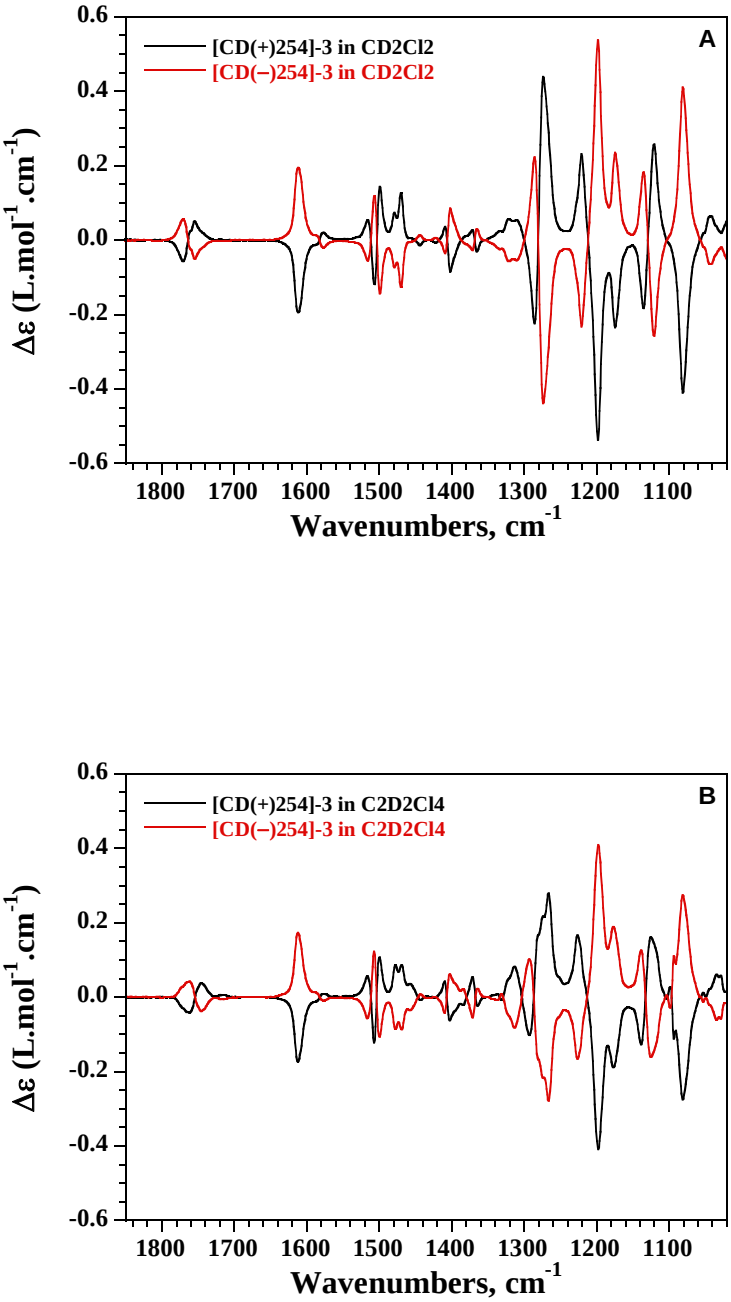

Figure S26: VCD spectra of [CD(+)$_{254}$]-**3** (black spectra) and [CD(−)$_{254}$]-**3** (red spectra) in a) CD_2Cl_2 and b) $C_2D_2Cl_4$ solvents (0.015 mM, 250 μm path length).

a) Optimized structure of *PP*-**1**: (IEFPCM = CH_2Cl_2)

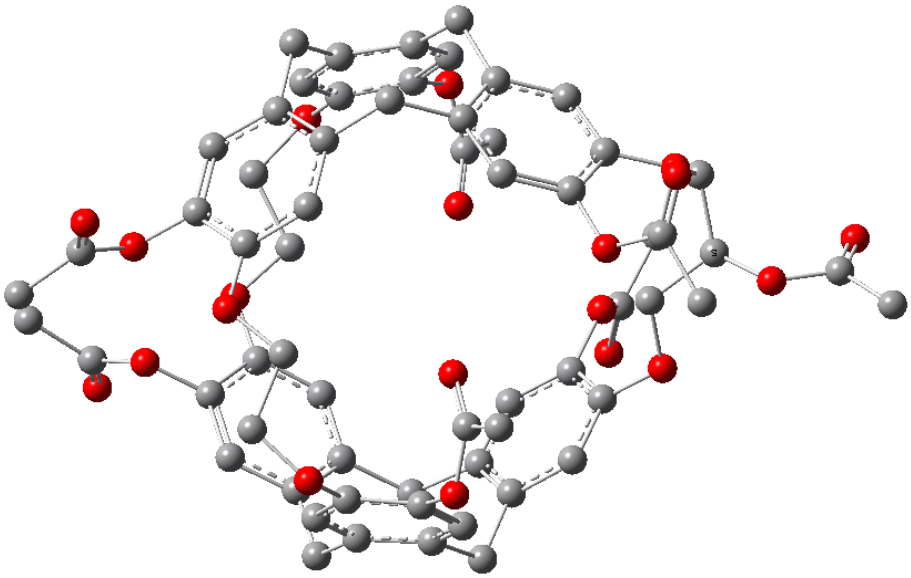

b) Optimized structure of *PP*-**1**: (IEFPCM = $C_2H_2Cl_4$)

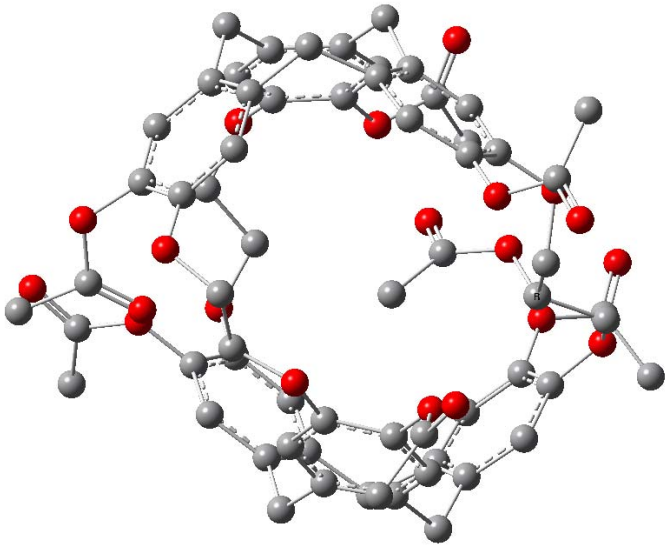

Figure S27: Optimized geometry of *PP*-**1** enantiomer calculated at the density functional theory (DFT) level using B3LYP functional and 6-31G** basis set with the use of IEFPCM model of solvent (IEFPCM = CH_2Cl_2 and $C_2H_2Cl_4$).

a) Optimized structure of *MM*-**2**: (IEFPCM = CH_2Cl_2)

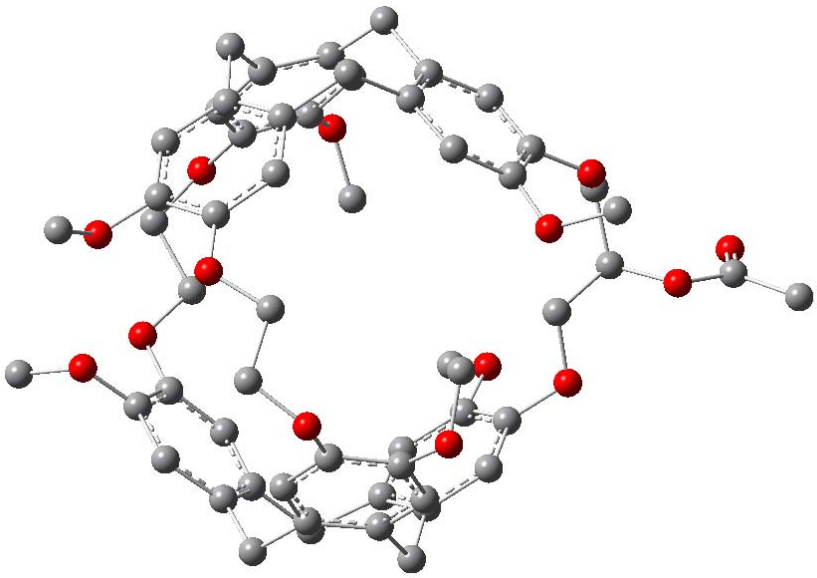

b) Optimized structure of *MM*-**2**: (IEFPCM = $C_2H_2Cl_4$)

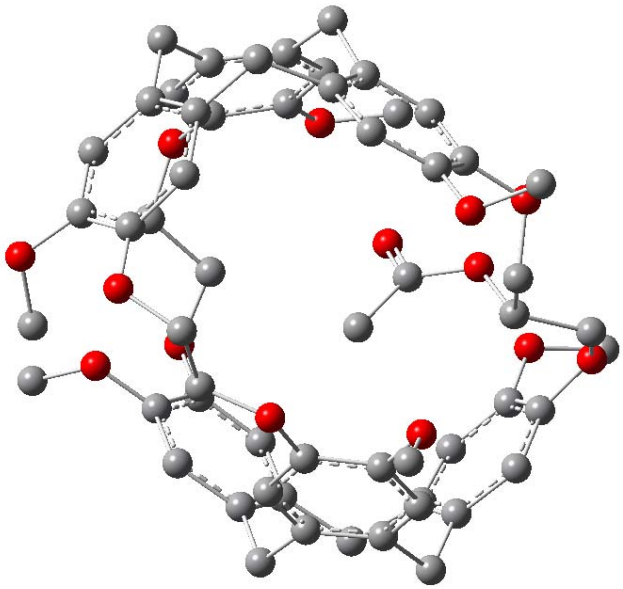

Figure S28: Optimized geometry of *MM*-**2** enantiomer calculated at the density functional theory (DFT) level using B3LYP functional and 6-31G** basis set with the use of IEFPCM model of solvent (IEFPCM = CH_2Cl_2 and $C_2H_2Cl_4$).

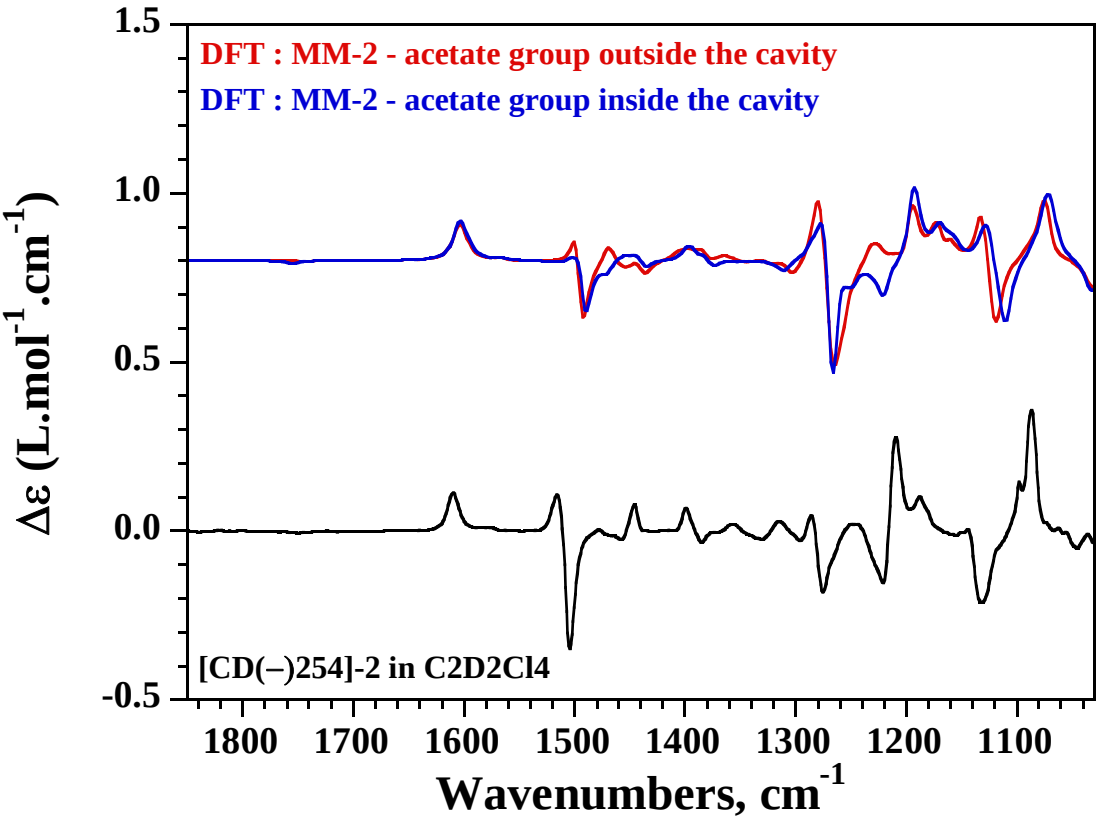

Figure S29: Comparison of experimental VCD spectrum of [CD(–)$_{254}$]-**2** in $C_2D_2Cl_4$ solution (15 mM, 250 µm path length) and VCD spectra of *MM*-**2** calculated at the B3LYP/6-31G** level (IEFPCM = $C_2H_2Cl_4$) for the *trans* and *gauche-gauche* conformations of the ethylenedioxy and propylenedioxy linkers, respectively, and for the acetate group grafted on the propylenedioxy linker pointing inside (blue spectrum) or outside (red spectrum) the cavity.

Table S1: Specific optical rotation values measured for [CD(+)$_{254}$]-**1** in different solvents at 25 °C.

Solvent	Conc.	$[\alpha]_{589}$	$[\alpha]_{577}$	$[\alpha]_{546}$	$[\alpha]_{435}$	$[\alpha]_{365}$
CH_2Cl_2	0.21	-60.1	-62.3	-70.3	-123.4	-190.9
$CHCl_3$	0.23	-25.4	-28.3	-32.1	-48.5	-59.8
DMSO	0.26	+7.2	+7.0	+8.0	+19.9	+61.4
$C_2H_2Cl_4$	0.26	+8.1	+9.1	+12.0	+23.4	+66.3

Table S2: Specific optical rotation values measured for [CD(–)$_{254}$]-**1** in different solvents at 25 °C.

Solvent	Conc.	$[\alpha]_{589}$	$[\alpha]_{577}$	$[\alpha]_{546}$	$[\alpha]_{435}$	$[\alpha]_{365}$
CH_2Cl_2	0.21	+58.4	+62.0	+70.3	+121.2	+188.2
$CHCl_3$	0.25	+23.9	+24.9	+28.4	+46.9	+57.3
DMSO	0.26	-7.6	-8.9	-9.7	-23.4	-66.1
$C_2H_2Cl_4$	0.29	-10.4	-9.8	-13.6	-26.2	-64.4

Table S3: Specific optical rotation values measured for [CD(+)$_{254}$]-**2** in different solvents at 25 °C.

Solvent	Conc.	$[\alpha]_{589}$	$[\alpha]_{577}$	$[\alpha]_{546}$	$[\alpha]_{435}$	$[\alpha]_{365}$
CH_2Cl_2	0.19	+159.0	+168.0	+194.5	+359.0	+664.5
$CHCl_3$	0.26	+201.0	+214.1	+246.5	+453.5	+845.1
DMSO	0.31	+228.3	+241.1	+278.8	+510.4	+943.5
$C_2H_2Cl_4$	0.21	+199.0	+213.0	+244.5	+448.0	+835.5

Table S4: Specific optical rotation values measured for [CD(–)$_{254}$]-**2** in different solvents at 25 °C.

Solvent	Conc.	$[\alpha]_{589}$	$[\alpha]_{577}$	$[\alpha]_{546}$	$[\alpha]_{435}$	$[\alpha]_{365}$
CH_2Cl_2	0.24	-155.0	-163.0	-189.0	-347.0	-652.0
$CHCl_3$	0.27	-200.2	-211.0	-245.0	-446.4	-823.4
DMSO	0.30	-227.8	-239.0	-276.4	-505.0	-936.0
$C_2H_2Cl_4$	0.20	-192.5	-206.0	-236.5	-440.5	-820.0

Table S5: Specific optical rotation values measured for [CD(+)$_{254}$]-**3** in different solvents at 25 °C.

Solvent	Conc.	$[\alpha]_{589}$	$[\alpha]_{577}$	$[\alpha]_{546}$	$[\alpha]_{435}$	$[\alpha]_{365}$
CH_2Cl_2	0.26	-66.0	-70.1	-78.7	-131.6	-191.3
$CHCl_3$	0.24	-38.6	-40.9	-47.3	-74.5	-90.4
DMSO	0.25	-50.0	-52.9	-60.5	-101.5	-145.0
DMF	0.27	-53.9	-54.8	-61.8	-102.6	-142.3
$C_2H_2Cl_4$	0.30	-38.9	-38.3	-45.7	-75.6	-112.7

Table S6: Specific optical rotation values measured for [CD(–)$_{254}$]-**3** in different solvents at 25 °C.

Solvent	Conc.	$[\alpha]_{589}$	$[\alpha]_{577}$	$[\alpha]_{546}$	$[\alpha]_{435}$	$[\alpha]_{365}$
CH_2Cl_2	0.25	+62.8	+64.5	+72.9	+122.0	+176.8
$CHCl_3$	0.29	+35.2	+38.0	+42.3	+68.0	+82.5
DMSO	0.26	+47.0	+49.0	+54.8	+92.2	+127.5
DMF	0.26	+45.3	+49.4	+55.0	+88.1	+118.5
$C_2H_2Cl_4$	0.31	+34.0	+35.1	+43.9	+68.2	+102.0

Table S7: B3LYP/6-31G** frequencies (scaled by 0.968) of the ester νC=O stretching vibration of *MM*-**2** (IEFPCM = CH_2Cl_2 and $C_2D_2Cl_4$) for the acetate group pointing inward or outward the cavity.

	IEFPCM = CH_2Cl_2	IEFPCM = $C_2D_2Cl_4$
Acetate pointing inward the cavity	1753.58	1755.17
Acetate pointing outward the cavity	1741.42	1742.52

Full list of authors of references 25

25 Frisch, M. J.; Trucks, G. W.; Schlegel, H. B.; Scuseria, G. E.; Robb, M. A.; Cheeseman, J. R.; Scalmani, G.; Barone, V.; Mennucci, B.; Petersson, G. A.; Nakatsuji, H.; Caricato, M.; Li, X.; Hratchian, H. P.; Izmaylov, A. F.; Bloino, J.; Zheng, G.; Sonnenberg, J. L.; Hada, M.; Ehara, M.; Toyota, K.; Fukuda, R.; Hasegawa, J.; Ishida, M.; Nakajima, T.; Honda, Y.; Kitao, O.; Nakai, H.; Vreven, T.; Montgomery, Jr., J. A.; Peralta, J. E.; Ogliaro, F.; Bearpark, M.; Heyd, J. J.; Brothers, E.; Kudin, K. N.; Staroverov, V. N.; Kobayashi, R.; Normand, J.; Raghavachari, K.; Rendell, A.; Burant, J. C.; Iyengar, S. S.; Tomasi, J.; Cossi, M.; Rega, N.; Millam, N. J.; Klene, M.; Knox, J. E.; Cross, J. B.; Bakken, V.; Adamo, C.; Jaramillo, J.; Gomperts, R.; Stratmann, R. E.; Yazyev, O.; Austin, A. J.; Cammi, R.; Pomelli, C.; Ochterski, J. W.; Martin, R. L.; Morokuma, K.; Zakrzewski, V. G.; Voth, G. A.; Salvador, P.; Dannenberg, J. J.; Dapprich, S.; Daniels, A. D.; Farkas, Ö.; Foresman, J. B.; Ortiz, J. V.; Cioslowski, J.; Fox, D. J. *Gaussian 09*, revision A.1, Gaussian Inc., Wallingford CT, **2009**.